Structures of *arachno*- and *hypho*-B_{10} Clusters and Stability of Their Possible Lewis Base Adducts ($[B_{10}H_{12}]^{2-}$, $[B_{10}H_{12}\cdot L]^{2-}$, $[B_{10}H_{12}\cdot 2L]^{2-}$, $[B_{10}H_{13}]^{-}$, $[B_{10}H_{13}\cdot L]^{-}$, $[B_{10}H_{12}\cdot 2L]$). An ab Initio/IGLO/NMR Investigation

Matthias Hofmann*,† and Paul von Ragué Schleyer†,‡

Center for Computational Quantum Chemistry, University of Georgia, 1004 Cedar Street,
Athens, Georgia 30602-2525, and Computer-Chemie-Centrum, Institut für Organische Chemie,
Universität Erlangen-Nürnberg, Henkestrasse 42, D-91052 Erlangen, Germany

Received May 20, 1998

The $[B_{10}H_{12}]^{2-}$ dianion has been shown by the ab initio/IGLO/NMR method to have a C_2 symmetric structure (**26**) derived from $B_{10}H_{14}$ (**17**) by removing two opposite bridge protons. Adduct formation with one or two solvent molecules, suggested on the basis of experimental NMR investigations, does not take place. $[B_{10}H_{12}\cdot nL]^{2-}$ ($n = 1, 2$) structures with various ligands are not bound (vs $[B_{10}H_{12}]^{2-}$ and n L) and do not reproduce the experimental ^{11}B NMR chemical shifts. The $[B_{10}H_{13}]^{-}$ structure (**19**), computed to have C_1 rather than C_s symmetry in solution (as in the solid state), also can be derived from $B_{10}H_{14}$ (**17**) by removal of a bridging proton. In both the mono- (**19**) and the dianion (**26**), a bridging hydrogen can rearrange easily from B5/B6 to B9/B10 (barrier ca. 5 kcal mol^{-1}) but not from B8/B9 to B9/B10 (barrier ca. 15 kcal mol^{-1}). The recently proposed 6,6-$(C_5H_5N)_2B_{10}H_{12}$ structure is not supported computationally.

Introduction

The stable *closo*-borane dianions, $[B_nH_n]^{2-}$, $n = 6-12$, adopt closed polyhedral cluster structures and are well characterized experimentally.[1] In contrast, relatively little is known about dianions derived from *nido*-, *arachno*-, or *hypho*-boranes. Experimental investigations on these classes of compounds are complicated by high reactivity toward, e.g., disproportionation, decomposition, and protonation. Consequently, non-*closo* dianions are ideal targets for computational studies which can complement these challenging experiments.

$[B_{10}H_{12}]^{2-}$ is a good example of such an extremely reactive species: only a few experimental results are available and they are contradictory. The first synthesis, achieved by reacting $B_{10}H_{14}$ (see Figure 5, **17**) with an excess of sodium hydride in diethyl ether, was reported by Wilkes and Carter in 1966.[2] A $B_{10}H_{14}$-like structure lacking bridging hydrogens but having the two "extra" hydrogen atoms of $[B_{10}H_{12}]^{2-}$ bound as *endo* terminal H's at B6 and B9 (C_{2v} symmetry) was proposed (see Figure 6, **22**). $[B_{10}H_{12}]^{2-}$ was used to synthesize metallaboranes; in contrast to the dianion itself, these complexes were amenable to X-ray structural analysis.[3] ^{11}B NMR data were reported by Greenwood and Youll in 1975 for the $[Ph_4As]_2$-$[B_{10}H_{12}]$ salt: δ −40.60 (1), −36.2 (1), −31.3, −25.9, −19.7 (total of 5), −6.65 (2), −1.44 (1).[4] This contradicts the 1966 (C_{2v}) structural proposal,[2] for which not more than four signals are expected. Recently Bridges and Gaines questioned the 1975 NMR work because they observed a quite different spectrum with only four ^{11}B signals (consistent with a C_{2v} symmetry) for $Na_2B_{10}H_{12}$ in THF.[5] The chemical shifts at δ −35.6 (2), −6.8 (4), −5.2 (2), and 5.3 (2) were assigned to B2,4, B5,7,8,10, B1,3, and B6,9, respectively, on the basis of $^{11}B-^{11}B$ COSY.[5,6] The absence of hydrogen bridges between B6 and B5,7 and between B9 and B8,10 was deduced because of the strong couplings between these sets of boron atoms. The yellow color of $M_2[B_{10}H_{12}]$ solutions in THF, MeCN, and DME (1,2-dimethoxyethane) was attributed to loose solvent−$[B_{10}H_{12}]^{2-}$ complexes. Likewise, the broad B6,9 signal was attributed to an interaction with solvent molecules at B6,9. The proposed structure considered to be the most favorable has two terminally bound *exo* donors L (MeCN or THF) and two hydrogens bridging B5/B10 and B7/B8 (static, C_{2v} symmetry). An alternative possibility, which also would be in line with the experimental findings, was mentioned: a fluxional system with only one donor ligand bound at B6 *or* at B9. Rapid equilibrium with free $[B_{10}H_{12}]^{2-}$ would lead to effective C_{2v} symmetry on the NMR time scale.

We have now applied the ab initio/IGLO/NMR method[7] to establish a different form as the solution structure of $[B_{10}H_{12}]^{2-}$ and to clarify the possible interaction with solvent molecules as well as the dynamic behavior. The investigation also includes related compounds, e.g., $[B_{10}H_{12}\cdot 2L]^{2-}$, $[B_{10}H_{12}\cdot 2L]$, $[B_{10}H_{12}\cdot L]^{2-}$, $[B_{10}H_{13}\cdot L]^{-}$ (L = Lewis base), and $[B_{10}H_{13}]^{-}$.

Computational Details

All geometries were fully optimized within the given symmetry consecutively at the HF/3-21G, HF/6-31G*, and MP2/6-31G* levels

---

† University of Georgia.

‡ Universität Erlangen-Nürnberg.

(1) (a) Lipscomb, W. N. *Boron Hydrides*; Benjamin: New York, 1963. (b) Muetterties, E. L. *Boron Hydride Chemistry*; Academic Press: New York, 1975.

(2) Wilkes, P. H.; Carter, J. C. *J. Am. Chem. Soc.* **1966**, *88*, 3441.

(3) Greenwood, N. N.; Ward, I. *Chem. Soc. Rev.* **1974**, *3*, 321.

(4) Greenwood, N. N.; Youll, B. *J. Chem. Soc., Dalton Trans.* **1975**, 158.

(5) Bridges, A. N.; Gaines, D. F. *Inorg. Chem.* **1995**, *34*, 4523.

(6) ^{11}B chemical shifts are not given explicitly in ref 5 but are estimated from the spectrum shown there.

(7) (a) Bühl, M.; Schleyer, P. v. R. *J. Am. Chem. Soc.* **1992**, *114*, 477. (b) Bühl, M.; Gauss, J.; Hofmann, M.; Schleyer, P. v. R. *J. Am. Chem. Soc.* **1993**, *115*, 12385. For an extensive list of references to ab initio/IGLO/NMR applications see: Diaz, M.; Jaballas, J.; Tran, D.; Lee, H.; Arias, J.; Onak, T. *Inorg. Chem.* **1996**, *35*, 4536.

10.1021/ic9805729 CCC: $15.00

of theory[8] using the Gaussian 94 program package.[9] Only valence electrons were considered for the electron correlation treatment (fc = frozen core approximation) in the MP2 procedure. Unless noted otherwise, MP2(fc)/6-31G* geometric parameters are reported. Harmonic frequencies were computed from analytical second derivatives at HF/6-31G* to establish the nature of stationary points. Relative energies at MP2/6-31G* are corrected for scaled (factor of 0.89) differences in HF/6-31G* zero-point vibrational energies (ZPE) (MP2-(fc)/6-31G* + 0.89 ZPE(HF/6-31G*)). Chemical shifts were computed using the IGLO method[10] at the SCF level employing Huzinaga's double-ζ (DZ) basis sets[11] in the recommended contraction schemes: (3s), [21] for H and (7s,3p), [4111,21] for B, C, and N. For the largest molecules, this was not possible and the GIAO−SCF[12] approach as implemented in the Gaussian program[9] was used instead together with the 6-31G* basis set. B_2H_6 ($\sigma = 114.88$ at IGLO/DZ and $\sigma = 106.98$ at GIAO−SCF/6-31G*) served as a primary reference for computed ^{11}B chemical shifts; the experimental gas-phase value of B_2H_6, $\delta = 16.6$,[13] was used to convert to the experimental standard, $BF_3{\cdot}OEt_2$ ($\delta = 0$).

Results and Discussion

$[B_{10}H_{12}{\cdot}L_2]^{2-}$. On the basis of experimental NMR results in solution, *nido*-$[B_{10}H_{12}]^{2-}$ was proposed to form a C_{2v} symmetric, static solvent adduct with two Lewis base molecules L (MeCN, THF) bound at B6 and B9.[5] Each donor L was supposed to contribute two electrons to the cluster bonding. Consequently, $[B_{10}H_{12}{\cdot}2L]^{2-}$ has a *hypho* electron count. The assumed structure, however, is typical for 10-vertex *arachno* clusters such as $[B_{10}H_{14}]^{2-}$, $B_{10}H_{12}{\cdot}2L$, or 6,9-$C_2B_8H_{14}$. Most of our computations modeled the donors L by HCN (unsaturated donor) or NH_3 (saturated) and assumed C_{2v}, C_s, or C_2 symmetry (see Figures 1−4).[14] For C_1 mimimum and C_s transition structures of $B_9H_{13}{\cdot}L$, we found only insignificant differences between L = MeCN and model HCN.[15] At HF/6-31G*, structure **1a** (Figure 1) corresponding to the [*exo*-6,*exo*-9-$L_2B_{10}H_{12}]^{2-}$ proposal has five (!) imaginary frequencies and is 149 kcal mol^{-1} higher in energy than two isolated HCN's and our best $[B_{10}H_{12}]^{2-}$ structure (**26**; see below). One (**2a**) or two (**3a**) *endo*-oriented ligands L also result in very high energy structures (relative energies of 122 and 147 kcal mol^{-1}, respectively). These complexes only can be computed at Hartree−Fock levels. Attempts to optimize **1a**−**3a** at the MP2/6-31G* electron-correlated level lead to dissociation or to cluster decomposition. When the ligands L were modeled by NH_3 instead of HCN, no minima corresponding to **1b**−**3b** could be located at correlated and even at noncorrelated levels. Computed ^{11}B chemical shifts for **1a** are in gross disagreement with the measured data (the difference is 44.7 ppm for B1,3; Table 1).[16]

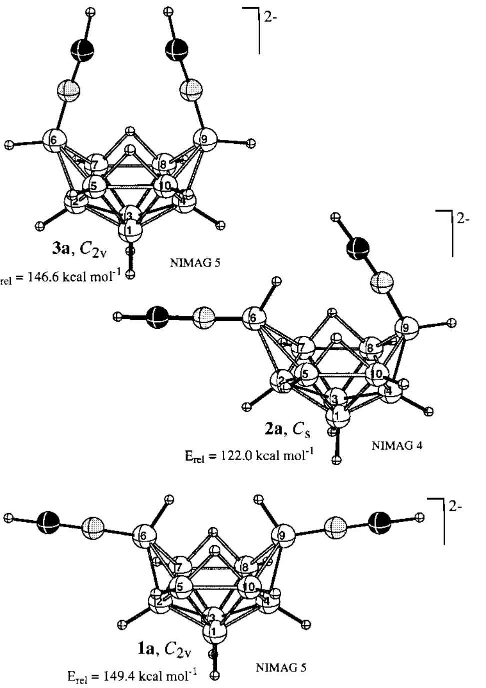

Figure 1. Optimized structures for $[6,9\text{-}(HCN)_2B_{10}H_{12}]^{2-}$ isomers. (Energies are given relative to isolated $[B_{10}H_{12}]^{2-}$, **26**, and HCN.)

Following the reviewers' suggestions, we also computed molecules with more realistic ligands, L (i.e., CH_3CN, $O(CH_3)_2$, and THF). The HF/6-31G* optimized geometry of [*exo*-6,*exo*-9-$(MeCN)_2B_{10}H_{12}]^{2-}$, **1c**, does not differ much from that of the HCN model compound. Chemical shifts obtained at GIAO−SCF/6-31G* also do not agree with the experimental data (see Table 1). While GIAO−SCF/6-31G* gives chemical shifts 5−10 ppm more positive compared to those at IGLO/DZ (for **1a**), the differences between the theoretical and measured data for **1c** are much larger (more than 40 ppm). Structure **1c** shows five imaginary frequencies (as does **1a**), and its relative energy vs two MeCN plus $[B_{10}H_{12}]^{2-}$ structure **26** (see below) is 155.4 kcal mol^{-1}, which is very close to the analogous value for **1a** (149.4 kcal mol^{-1}). With L = $O(CH_3)_2$ and THF, optimizations of [*exo*-6,*exo*-9-$L_2B_{10}H_{12}]^{2-}$ starting geometries (with C_{2v} and C_2 symmetry contraints, respectively) lead either to dissociation into $[B_{10}H_{12}]^{2-}$ and 2 L or (for L = THF) to transfer of electrons and THF ring opening. The latter process results in two extra electrons on the ligands L, and the species produced thus has to be considered as an *arachno*-$[(L^-)_2{\cdot}B_{10}H_{12}]$ compound in line with electron-counting rules (rather than as a *hypho*-$[L_2{\cdot}B_{10}H_{12}]^{2-}$ compound).

All these computational results contradict the proposal that a $[B_{10}H_{12}{\cdot}2L]^{2-}$ species exists in solution.[5]

$[B_{10}H_{12}{\cdot}2L]$. Structures akin to **1a**, on the other hand, are well established for *arachno* species such as neutral $B_{10}H_{12}{\cdot}2L$ or the $[B_{10}H_{14}]^{2-}$ dianion (**4**). In 1957, Schaeffer reported the first example of a $B_{10}H_{12}{\cdot}2L$ species (L = MeCN).[17] The *exo*-6,*exo*-9-$(MeCN)_2B_{10}H_{12}$ structure (**5c**) was determined by an

---

(8) For an introduction to computational chemistry and the usual nomenclature see: (a) Foresman, J. B.; Frisch, Æ. *Exploring Chemistry with Electronic Structure Methods. A Guide to Using Gaussian*; Gaussian Inc.: Pittsburgh, PA, 1993. (b) Hehre, W. J.; Radom, L.; Schleyer, P. v. R.; Pople, J. A. *Ab initio Molecular Orbital Theory*; Wiley: New York, 1986.

(9) Frisch, M. J.; Trucks, G. W.; Schlegel, H. B.; Gill, P. M. W.; Johnson, B. G.; Robb, M. A.; Cheeseman, J. R.; Keith, T.; Petersson, G. A.; Montgomery, J. A.; Raghavachari, K.; Al-Laham, M. A.; Zakrzewski, V. G.; Ortiz, J. V.; Foresman, J. B.; Cioslowski, J.; Stefanov, B. B.; Nanayakkara, A.; Challacombe, M.; Peng, C. Y.; Ayala, P. Y.; Chen, W.; Wong, M. W.; Andres, J. L.; Replogle, E. S.; Gomperts, R.; Martin, R. L.; Fox, D. J.; Binkley, J. S.; Defrees, D. J.; Baker, J.; Stewart, J. P.; Head-Gordon, M.; Gonzalez, C.; Pople, J. A. *Gaussian 94*, Revision C.3; Gaussian, Inc.: Pittsburgh, PA, 1995.

(10) (a) Kutzelnigg, W. *Isr. J. Chem.* **1980**, *19*, 193. (b) Schindler, M.; Kutzelnigg, W. *J. Chem. Phys.* **1982**, *76*, 1919. (c) Kutzelnigg, W.; Fleischer, U.; Schindler, M. *NMR* **1990**, *23*, 165.

(11) Huzinaga, S. *Approximate Atomic Wave Functions*; University of Alberta: Edmonton, Canada, 1971.

(12) (a) London, F. *J. Phys. (Paris)* **1937**, *8*, 397. (b) Wolinski, K.; Hilton, J. F.; Pulay, P. *J. Am. Chem. Soc.* **1990**, *112*, 8251.

(13) Onak, T. P.; Landesman, H. L.; Williams, R. E. *J. Phys. Chem.* **1959**, *63*, 1533.

(14) For structures with donor molecules L coordinated to boron hydride clusters, we use the following labels: **a**, L = NCH; **b**, L = NH_3; **c**, L = $NCCH_3$; **d**, L = pyridine.

(15) Hofmann, M.; Schleyer, P. v. R. *Inorg. Chem.*, in press.

(16) The IGLO procedure did not converge for **2a** and **3a**.

(17) Schaeffer, R. *J. Am. Chem. Soc.* **1957**, *79*, 1006.

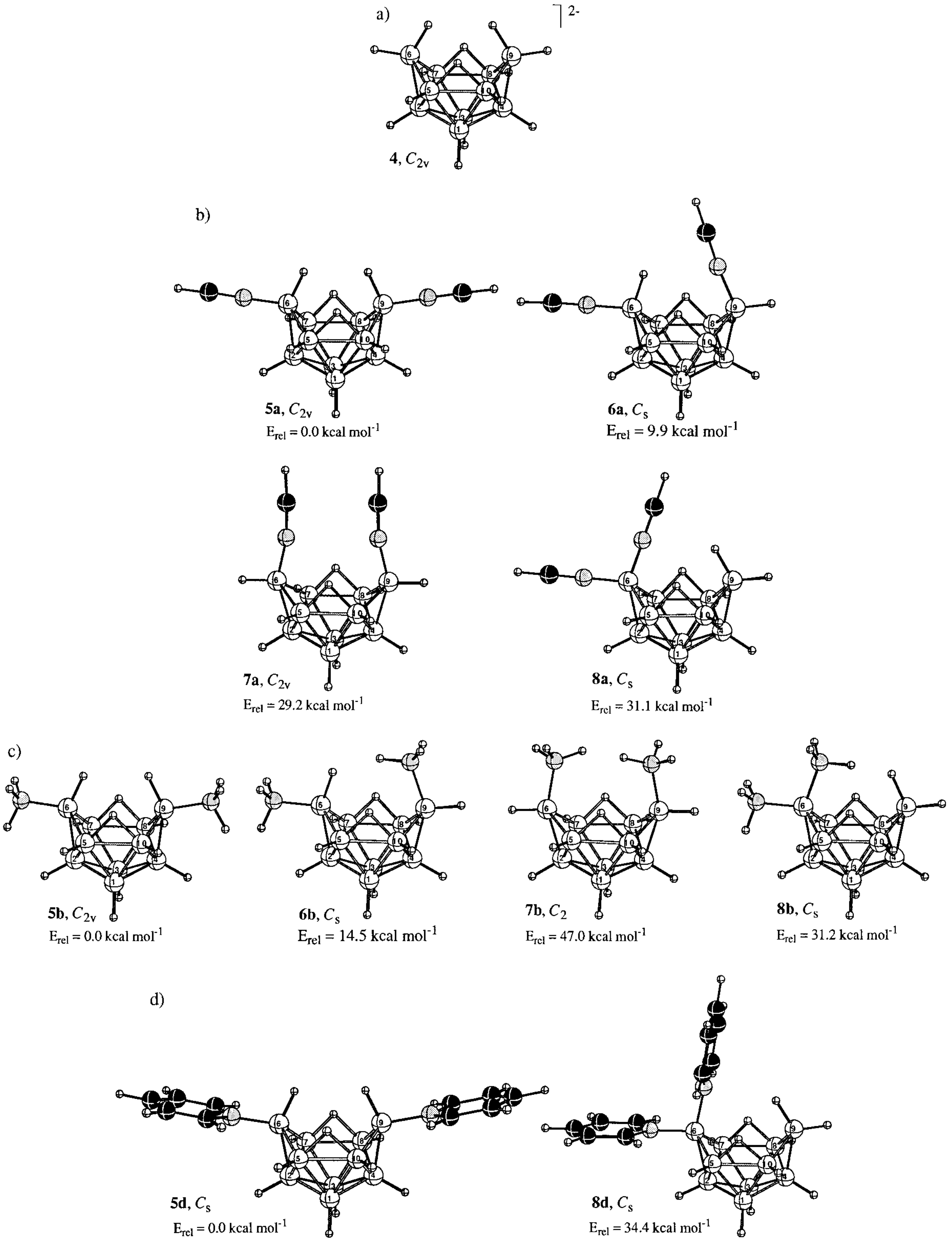

4, C_{2v}

5a, C_{2v} $E_{rel} = 0.0$ kcal mol^{-1}

6a, C_s $E_{rel} = 9.9$ kcal mol^{-1}

7a, C_{2v} $E_{rel} = 29.2$ kcal mol^{-1}

8a, C_s $E_{rel} = 31.1$ kcal mol^{-1}

5b, C_{2v} $E_{rel} = 0.0$ kcal mol^{-1}

6b, C_s $E_{rel} = 14.5$ kcal mol^{-1}

7b, C_2 $E_{rel} = 47.0$ kcal mol^{-1}

8b, C_s $E_{rel} = 31.2$ kcal mol^{-1}

5d, C_s $E_{rel} = 0.0$ kcal mol^{-1}

8d, C_s $E_{rel} = 34.4$ kcal mol^{-1}

Figure 2. *arachno*-$[B_{10}H_{14}]^{2-}$, **4** (a), and related $B_{10}H_{12}\cdot 2L$ isomers with L = HCN (b), L = NH_3 (c), or L = pyridine (d).

X-ray structure analysis.[18] ^{11}B NMR data[19] agree reasonably well with the values computed for *exo*-6,*exo*-9-$(HCN)_2B_{10}H_{12}$ (**5a**), C_{2v} (Table 3). This demonstrates that the MeCN ligand is modeled well by HCN: The computed ^{11}B chemical shifts differ by less than 1 ppm. The computational level (IGLO or GIAO) has a larger influence (differences in chemical shifts of 2−4 ppm with GIAO−SCF to higher field).

Most $B_{10}H_{12}\cdot 2L$ molecules known experimentally are derived formally from *arachno*-$[B_{10}H_{14}]^{2-}$, **4**, by replacing *exo* terminal hydrides H^- at B6 and B9 by Lewis bases L. Recently, a 6,6-$(py)_2B_{10}H_{12}$ (py = pyridine, NC_5H_5) complex, with geminal ligands, also was proposed on the basis of NMR investigations

---

(18) (a) van der Maas Reddy, J.; Lipscomb, W. N. *J. Am. Chem. Soc.* **1959**, *81*, 754. (b) van der Maas Reddy, J.; Lipscomb, W. N. *J. Chem. Phys.* **1959**, *31*, 610.

(19) Hyatt, D. E.; Scholer, F. R.; Todd, L. J. *Inorg. Chem.* **1967**, *6*, 630.

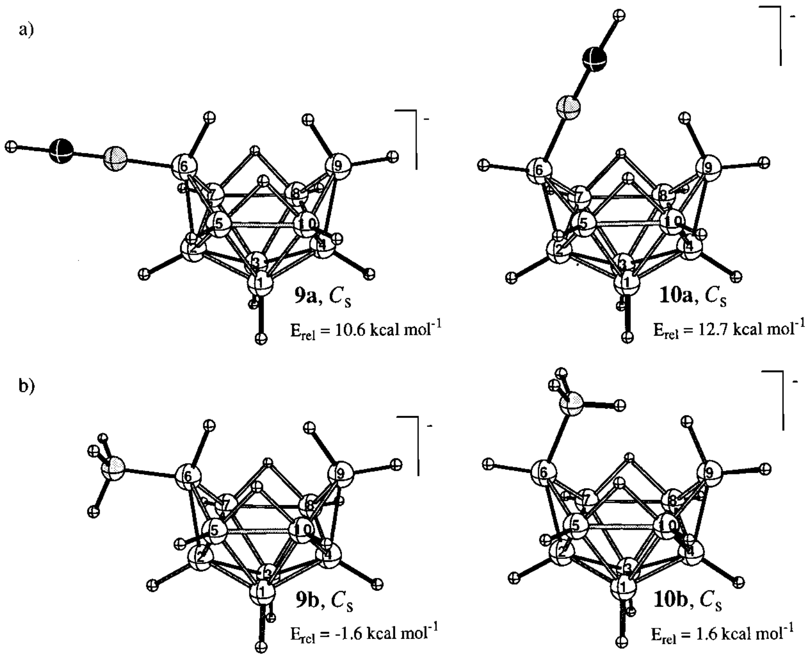

Figure 3. Optimized structures of *exo*- and *endo*-[6-$LB_{10}H_{13}$]$^{-}$ isomers. (Energies are given relative to isolated [$B_{10}H_{12}$]$^{2-}$, **26**, and HCN.)

(2D $^{11}B-^{11}B$ COSY and pure-phase $^{11}B-^{11}B$ 2Q correlation NMR) and characterized by FTIR, UV−vis, mass spetroscopy, and elemental analysis.[20] While computational models 6,6-$L_2B_{10}H_{12}$, **8a** (L = HCN) and **8b** (L = NH_3), are minima, these are ca. 31 kcal mol^{-1} higher in energy than the *exo,exo* isomers, **5a** and **5b**, respectively. For the pyridine ligand, the energy difference between **5d** and **8d** is 34.5 kcal mol^{-1}. This is in line with the experimental observation that **8d** is rapidly converted into its isomer **5d** when refluxed. Compound **8d** may have been formed by kinetic control. Chemical shifts computed for models **8a** and **8b** do not compare well with the experimental data assigned to 6,6-$(py)_2B_{10}H_{12}$ (see Table 3). Computations (GIAO−SCF/6-31G* chemical shifts on HF/6-31G* and B3LYP/6-31G* optimized geometries) on 6,6-$(py)_2B_{10}H_{12}$, **8d**, do not not agree satisfactorily, either. However, a comparison of experimental and computed chemical shifts for the *exo*-6,*exo*-9 isomer, **5d**, also shows unusually large differences of up to almost 11 ppm. A large part of this deviation is likely due to the computational level as can be judged from IGLO and GIAO results for model compounds (compare Tables 1−3). For **8d**, however, the discrepancies between theoretical and experimental results are as much as 21 ppm, twice as large as is usual at this level. Unfortunately, due to the sizes of the molecules **5d** and **8d**, we are not able to apply IGLO/DZ//MP2(fc)/6-31G*, our method of choice, which would give more reliable results. Nevertheless, the computed chemical shifts raise some doubts about the validity of the 6,6-substituted 2L·$B_{10}H_{12}$ structural proposal although we cannot discard it with certainty on the basis of our results.

We find the following stability order for neutral $(HCN)_2B_{10}H_{12}$: *exo*-6,*exo*-9 (**5a**) > *exo*-6,*endo*-9 (**6a**) > *endo*-6,*endo*-9 (**7a**) ≈ *exo*-6,*endo*-6 (**8a**) (see Figure 2). For L = NH_3, the relative energies are about the same but the *endo*-6,*endo*-9 isomer is much less stable most likely due to enhanced steric repulsion involving the more crowded NH_3 ligands.

[$B_{10}H_{13}$·L]$^{-}$. Experimentally, a derivative of [$B_{10}H_{14}$]$^{2-}$ with only one H^{-} replaced by a neutral L has been reported to form in the reaction of [$B_{10}H_{13}$]$^{-}$ with $NHEt_2$.[21] The resulting *arachno*-[$B_{10}H_{13}$·L]$^{-}$ monoanion (L = $NHEt_2$) was postulated to be "structurally equivalent to $B_{10}H_{12}$·2L compounds (e.g., **5a**) except that one ligand is replaced by a hydride anion". To our knowledge, only a very poorly resolved ^{11}B NMR spectrum has been reported (in 1962)[21] showing three resonances at −14.4, −36.6, and −47.1 ppm.[22] Unfortunately, the poor quality of the data prevents a [$B_{10}H_{13}$·$NHEt_2$]$^{-}$ structure determination by the ab initio/IGLO/NMR method.

Table 1. ^{11}B Chemical Shifts (ppm) for [*Exo*-6,*Exo*-9-$L_2B_{10}H_{12}$]$^{2-}$

	B1,3	B2,4	B5,7,8,10	B6,9
1a: L = NCH^{a,c}	−49.9	−50.7	−5.2	3.9
1a: L = NCH^{b,c}	−45.1	−42.7	0.0	14.6
1c: L = NCMe^{b,c}	−45.0	−38.1	−3.8	−5.7
1c: L = NCMe^{b,d}	−47.6	−35.7	−7.8	−7.8
experiment^{e}	*−5.2*	*−35.6*	*−6.8*	*5.3*

[a] IGLO/DZ. [b] GIAO−SCF/6-31G*. [c] //HF/6-31G*. [d] //B3LYP/6-31G*. [e] Experimental data for [$B_{10}H_{12}$]$^{2-}$ in solution; values have been estimated from the spectra shown in ref 5.

[*exo*-6-$LB_{10}H_{13}$]$^{-}$ is only favored slightly over the *endo* isomer. The difference in energy is 2.1 kcal mol^{-1} for L = HCN (**9a**/**10a**) and 3.2 kcal mol^{-1} for L = NH_3 (**9b**/**10b**). This contrasts the $B_{10}H_{12}$·2L situation where the *exo* preference is much more pronounced (see above and Figure 2). Hence, *endo* substitution is easier to achieve in the presence of only one L. On the other hand, the energy of **9a** is +10.6 kcal mol^{-1} higher than that of isolated HCN and [$B_{10}H_{13}$]$^{-}$ (**19**; Figure 5). The amino adduct **9b** is bound but only slightly (by 1.6 kcal mol^{-1}). As observed for $B_{10}H_{12}$·2L, the resonance of the B6 ipso boron atom is most sensitive to the *exo*/*endo* orientation of L (Table 4). For *exo*-L, the B6 chemical shift is found at ca. 8−10 ppm higher field than *endo*-oriented L. Redetermination of the ^{11}B NMR spectrum should allow *exo*- and *endo*-[6-$LB_{10}H_{13}$]$^{-}$ to be distinguished by comparison with the theoretical predictions.

---

(20) Cendrowski-Guillaume, S. M.; O'Laughlin, J. L.; Pelczer, I.; Spencer, J. T. *Inorg. Chem.* **1995**, *34*, 3935.

(21) Graybill, B. M.; Pitochelli, A. R.; Hawthorne, M. F. *Inorg. Chem.* **1962**, *1*, 622.

(22) A value of 18.1 ppm was used to convert from the old, $B(OMe)_3$, to the new standard BF_3·OEt_2. (Hermánek, S. *Chem. Rev.* **1992**, *92*, 325).

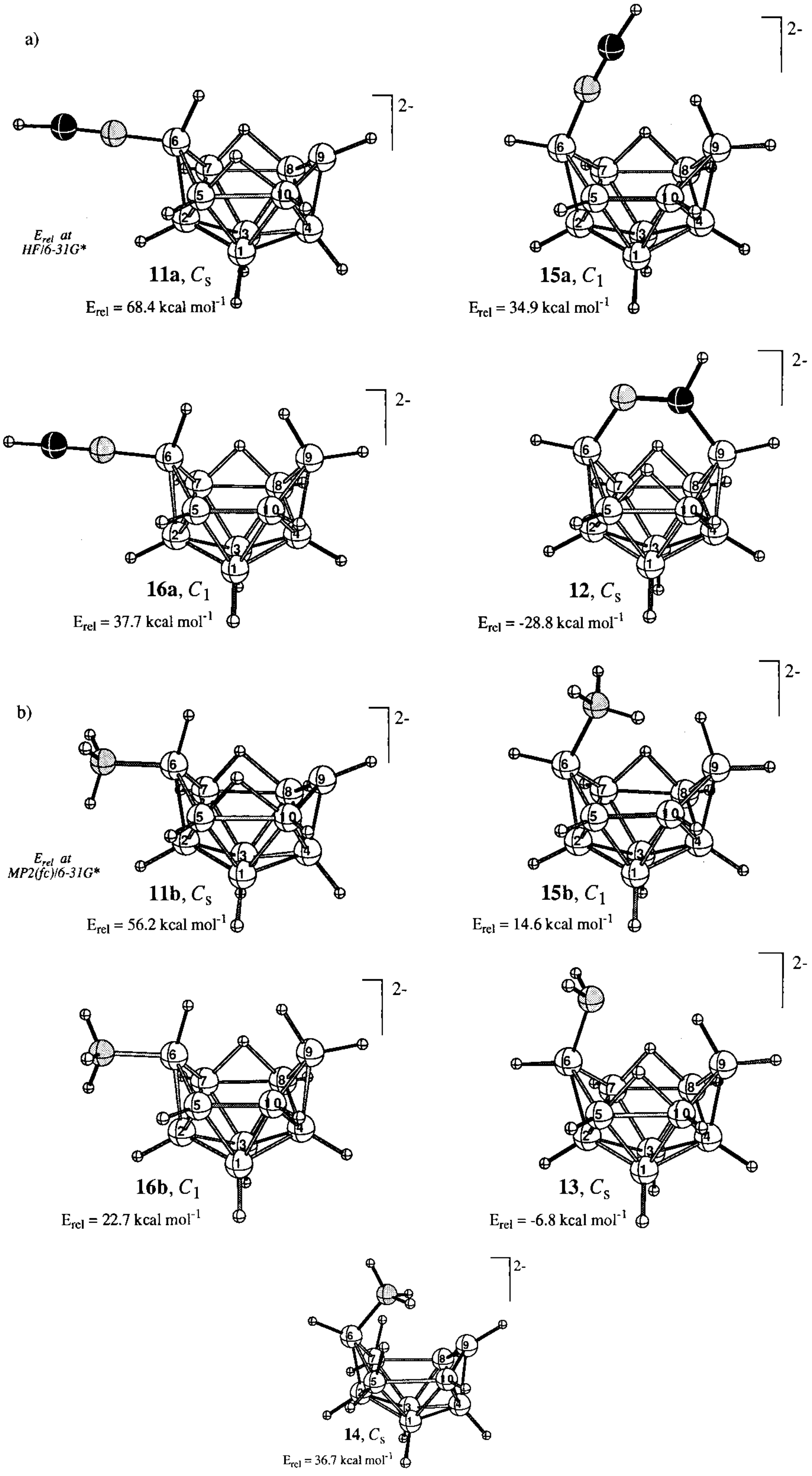

11a, C_s
E_{rel} = 68.4 kcal mol^{-1}

15a, C_1
E_{rel} = 34.9 kcal mol^{-1}

16a, C_1
E_{rel} = 37.7 kcal mol^{-1}

12, C_s
E_{rel} = -28.8 kcal mol^{-1}

11b, C_s
E_{rel} = 56.2 kcal mol^{-1}

15b, C_1
E_{rel} = 14.6 kcal mol^{-1}

16b, C_1
E_{rel} = 22.7 kcal mol^{-1}

13, C_s
E_{rel} = -6.8 kcal mol^{-1}

14, C_s
E_{rel} = 36.7 kcal mol^{-1}

Figure 4. Optimized structures of $[L{\cdot}B_{10}H_{12}]^{2-}$ isomers. (Energies are given relative to $[B_{10}H_{12}]^{2-}$, **26**, and HCN (a) and NH_3 (b), respectively.)

$[B_{10}H_{12}\ {\cdot}L]^{2-}$. Rapid equilibria (eq 1) have been suggested as an alternative explanation for the NMR spectroscopic findings on $[B_{10}H_{12}]^{2-}$ in solution.[5] $[B_{10}H_{12}{\cdot}L]^{2-}$ has an *arachno* electron count, and the prototype *arachno*-B_{10} cluster structure corresponds to $[B_{10}H_{14}]^{2-}$ (**4**). In **11a** (Figure 4), one *endo*-H of **4** (at B9) is removed while the *exo*-H at B6 is replaced by a Lewis donor L (HCN). This arrangement was suggested for $[B_{10}H_{12}{\cdot}L]^{2-}$ in ref 5, but it is 63 kcal mol^{-1} (MP2(fc)/6-31G*) higher in energy than $[B_{10}H_{12}]^{2-}$ (**26**; see Figure 6) and a

$$[exo\text{-}6\text{-}LB_{10}H_{12}]^{2-} \rightleftharpoons L + [B_{10}H_{12}]^{2-} \rightleftharpoons [exo\text{-}9\text{-}LB_{10}H_{12}]^{2-} \quad (1)$$

Table 2. ^{11}B Chemical Shifts (ppm) for $[L{\cdot}B_{10}H_{12}]^{2-}$ [a]

	B1,3	B2	B4	B5,7	B6	B8,10	B9
11a: *exo*-6, L = NCH	−39.8	−11.3	−26.2	−42.8	−36.0	−14.9	−4.9
11a: *exo*-6, L = NCH, av	−39.8	−18.7	−18.7	−28.8	−20.5	−28.8	−20.5
11a: *exo*-6, L = NCH[b]	−34.1	−6.8	−22.3	−37.2	−32.1	−12.8	−6.1
11b: *exo*-6, L = NH_3	−39.9	−9.2	−36.2	−55.9	−21.2	−13.1	−7.2
11b: *exo*-6, L = NH_3, av	−39.9	−22.7	−22.7	−34.5	−14.2	−34.5	−14.2
11c: *exo*-6, L = NCMe[b]	−34.5	−6.6	−23.7	−39.3	−31.3	−12.8	−7.0
11c: *exo*-6, L = NCMe, av[b]	−34.5	−15.2	−15.2	−26.1	−19.2	−26.1	−19.2
12: 6,9-bridging, L = NCH	−32.1	−5.4	−9.8	−21.0	−9.3	−18.9	−23.0
13: *endo*-6-NH_2, *endo*-9-H	−27.3	23.3	18.4	−7.5	2.5	−0.4	−21.1
14: *endo*-6, L = NH_3	−11.9	−13.2	−32.1	−30.7	3.1	16.5	10.8
15a: *exo*-6, L = NCH[c]	−39.9, −45.5	−2.5	−3.6	−12.9, −26.5	−36.3	−27.2, −10.3	−35.0
15a: *exo*-6, L = NCH, av[c]	−42.7	−3.1	−3.1	−19.2	−35.7	−19.2	−35.7
15b: *exo*-6, L = NH_3	−41.9, −46.4	−0.6	−9.7	−20.4, −33.5	−26.8	−29.4, −9.7	−39.0
15b: *exo*-6, L = NH_3, av	−44.2	−5.2	−5.2	−23.3	−32.9	−23.3	−32.9
16a: *endo*-6, L = NCH[c]	−37.3, −37.1	3.5	0.3	−6.7, −24.3	−31.7	−27.8, −2.4	−31.3
16a: *endo*-6, L = NCH, av[c]	−37.2	1.9	1.9	−15.3	−31.5	−15.3	−31.5
16b: *endo*-6, L = NH_3	−33.2, −40.4	7.0	2.0	−8.8, −28.4	−23.9	−19.0, −15.4	−39.0
16b: *endo*-6, L = NH_3, av	−36.8	4.5	4.5	−17.9	−31.5	−17.9	−31.5
experiment[d]	*−5.2*	*−35.6*	*−35.6*	*−6.8*	*5.3*	*−6.8*	*5.3*

[a] Computational level is IGLO/DZ//MP2(fc)/6-31G* if not specified otherwise. [b] GIAO−SCF/6-31G* [c] //HF/6-31G*. [d] Experimental data for $[B_{10}H_{12}]^{2-}$ in solution; values have been estimated from the spectra shown in ref 5.

Table 3. ^{11}B Chemical Shifts (ppm) for *arachno*-$B_{10}H_{12}{\cdot}2L$ Complexes[a]

	B1,3	B2	B4	B5,7	B6	B8,10	B9
5a: *exo*-6,*exo*-9; L = HCN	−41.0	1.9	1.9	−18.5	−31.6	−18.5	−31.6
5a: *exo*-6,*exo*-9; L = HCN[b]	−37.2	5.0	5.0	−15.2	−29.7	−15.2	−29.7
5b: *exo*-6,*exo*-9; L = NH_3	−43.2	−0.8	−0.8	−22.0	−27.8	−22.0	−27.8
5c: *exo*-6,*exo*-9; L = MeCN[b]	−37.8	4.2	4.2	−16.1	−29.3	−16.1	−29.3
5c: *exo-6,exo-9;* L = *MeCN, expt*[c]	*−42.8*	*−5.7*	*−5.7*	*−20.4*	*−31.2*	*−20.4*	*−31.2*
5d: *exo*-6,*exo*-9; L = pyridine[b,d]	−39.0	3.9	3.9	−17.9	−16.7	−17.9	−16.7
5d: *exo-6,exo-9;* L = *pyridine, expt*[e]	*−40.3*	*−5.3*	*−5.3*	*−19.0*	*−27.5*	*−19.0*	*−27.5*
6a: *exo*-6,*endo*-9; L = HCN	−35.9	7.3	8.7	−14.1	−30.1	−15.0	−23.4
6b: *exo*-6,*endo*-9; L = NH_3	−37.5	9.7	10.8	−15.1	−26.8	−19.3	−14.0
7a: *endo*-6,*endo*-9; L = HCN	−31.6	18.6	18.6	−9.4	−20.9	−9.4	−20.9
7b: *endo*-6,*endo*-9; L = NH_3	−30.2	23.5	23.5	−17.7, −6.8	−26.5	−17.7, −6.8	−26.5
8a: *exo*-6,*endo*-6; L = HCN[f]	−35.1	1.2	7.3	−8.5	−22.6	−16.5	−14.2
8b: *exo*-6,*endo*-6; L = NH_3	−35.3	12.7	8.9	−19.4	−16.4	−14.6	−21.4
8d: *exo*-6,*endo*-6; L = pyridine[b,g]	−29.5	19.7	9.7	−16.2	6.3	−8.8	−22.1
8d: *exo*-6,*endo*-6; L = pyridine[b,d]	−30.3	18.1	8.6	−16.4	4.6	−10.5	−23.1
8d: *exo-6,endo-6*; L = *pyridine, expt*[e]	*−38.1*	*−3.3*	*−4.8*	*−17.1*	*−17.1*	*−19.2*	*−29.4*

[a] Computational level is IGLO/DZ//MP2(fc)/6-31G* unless specified otherwise. [b] GIAO−SCF/6-31G*. [c] Reference 19. [d] //B3LYP/6-31G*. [e] Reference 20. [f] HCN moieties were constrained to be linear. [g] //HF/6-31G*.

Table 4. ^{11}B Chemical Shifts (ppm) for *arachno*-$[B_{10}H_{13}{\cdot}L]^-$ [a]

	B1,3	B2	B4	B5,7	B6	B8,10	B9
9a: *exo*-6, L = HCN	−41.4	−3.1	−0.7	−16.5	−37.3	−22.9	−26.5
9b: *exo*-6, L = NH_3	−43.1	0.0	−3.9	−23.4	−29.1	−22.2	−30.8
10a: *endo*-6, L = HCN	−36.3	2.2	3.2	−12.5	−29.1	−19.7	−23.8
10b, *endo*-6, L = NH_3	−37.6	8.4	5.5	−19.7	−19.5	−16.1	−30.4
exo-6, L = *$NHEt_2$, expt*[b]	*−47.0, −14.3, −36.5*[b]						
4: L = H^-	−43.8	−4.3	−4.3	−23.5	−36.4	−23.5	−36.4
4: L = *H^-, expt*[c]	*−42.26*	*−8.09*	*−8.09*	*−23.10*	*−36.62*	*−23.1*	*−36.62*

[a] Computed at IGLO/DZ//MP2(fc)/6-31G*. [b] Reference 21; without assignment. [c] Reference 30.

dissociated HCN molecule. For L = MeCN and NH_3, the differences are similar: 65.1 (**11c** vs $[B_{10}H_{12}]^{2-}$ (**26**) and MeCN) and 56.2 kcal mol^{-1} (**11b** vs $[B_{10}H_{12}]^{2-}$ (**26**) and NH_3).

In view of these energetic relationships, [*exo*-6-$LB_{10}H_{12}]^{2-}$ species are very unlikely to be present in solution in significant amounts. In addition, computed chemical shifts for **11a**, averaged to C_{2v} symmetry according to a hypothetical [*exo*-6-$LB_{10}H_{12}]^{2-}$/[*exo*-9-$LB_{10}H_{12}]^{2-}$ equilibrium (eq 1), differ considerably (up to 34.6 ppm for B1) from experimental data. GIAO-computed chemical shifts for **11c** differ somewhat from the IGLO values for **11a**, but this is more likely to be due to the performance of different levels of theory rather than to the different L's. This is indicated by the GIAO values for **11a**. A different ligand, e.g., NH_3 (**11b**) influences the chemical shift not only of the ipso boron atom, B6 ($\Delta\delta = +15$ ppm), but also of B4 ($\Delta\delta = -10$ ppm) and B5,7 ($\Delta\delta = -13$ ppm) strongly;

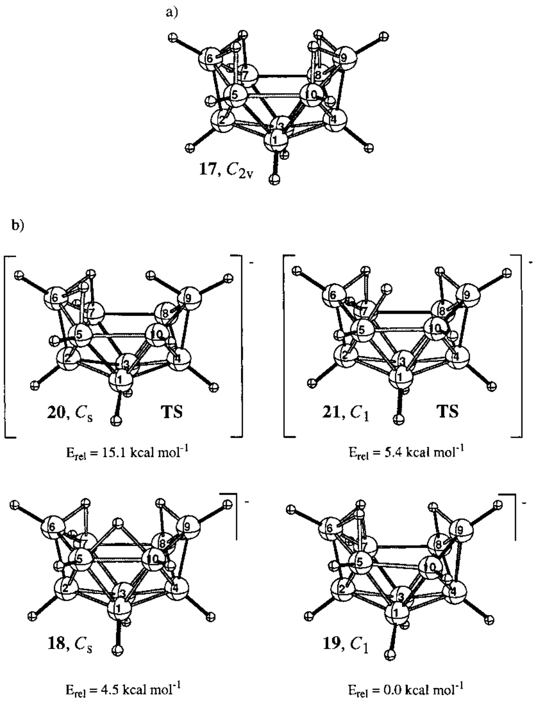

Figure 5. Optimized structures (a) for *nido*-$B_{10}H_{14}$ (**17**) and (b) for the corresponding *nido*-$[B_{10}H_{13}]^-$ monoanion (**18**−**21**).

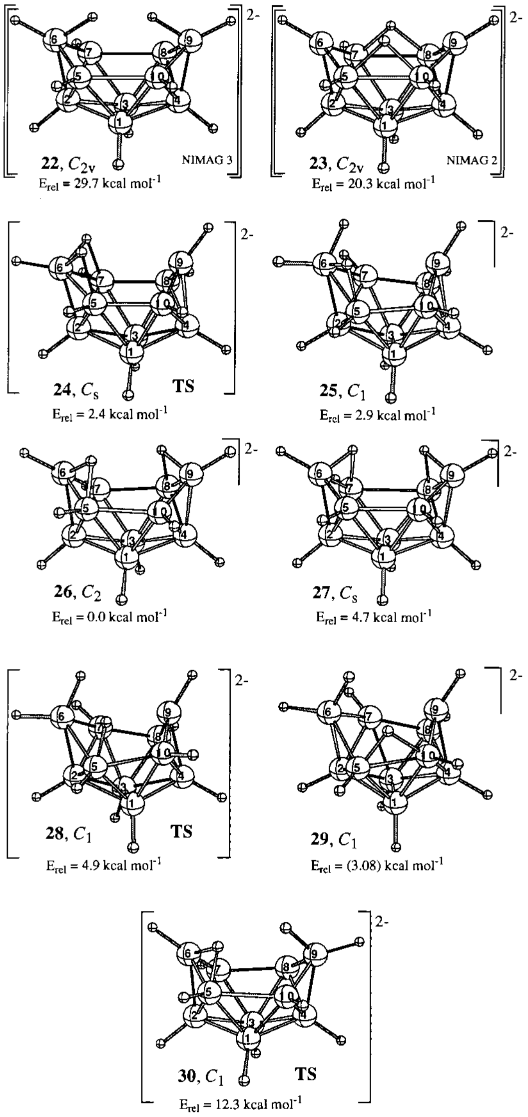

Figure 6. Optimized structures for *nido*-$[B_{10}H_{12}]^{2-}$.

however, the discrepancy with the experimental data also is large. All attempts to optimize an $[exo\text{-}6\text{-}(THF)B_{10}H_{12}]^{2-}$ geometry were unsuccessful since dissociation into $[B_{10}H_{12}]^{2-}$ and THF occurred. In conclusion, relative energies and chemical shift considerations are contradicting the proposed equilibrating $[exo\text{-}6\text{-}LB_{10}H_{12}]^{2-}$ solution structure.[5]

An $[endo\text{-}6\text{-}(HCN)B_{10}H_{12}]^{2-}$ starting geometry converged to **12** upon optimization. The HCN unit in **12** is bound as a 6,9-bridging moiety (−HC═N−) substituting both *endo*-H's of **4** (at B6 and B9) rather than as a terminal ligand (H−C≡N|). The structure thus represents a "normal" *arachno* cluster and is 107.8 kcal mol^{-1} (MP2(fc)/6-31G*) more stable than $[exo\text{-}6\text{-}(HCN)B_{10}H_{12}]^{2-}$, **11a**.

The amino ligand L = NH_3 should not bridge and was investigated as a model for an $[endo\text{-}6\text{-}LB_{10}H_{12}]^{2-}$ species. However, a starting geometry with one NH_3 hydrogen atom pointing *endo* toward B9 led on optimization to H-transfer from N to B9 without a barrier. The resulting structure **13** again represents a **4**-like *arachno*-B_{10} cluster with an *endo*-NH_2 substituent at B6. The energy of **13** is 62.9 kcal mol^{-1} lower than that of $[exo\text{-}6\text{-}(NH_3)B_{10}H_{12}]^{2-}$, **11b**.

A different C_s starting geometry with one N−H bond eclipsing B6−H*exo* does not allow a single H to move from N to B9. Optimization gave the strange-looking transition structure for NH_3 rotation, **14**, with *endo*-H's at B5 and B7. Although much higher in energy than **13**, **14** is even 19.4 kcal mol^{-1} lower in energy than **11b** (which was proposed originally).[5]

$[L\cdot B_{10}H_{12}]^{2-}$ can be considered to be a deprotonated $[L\cdot B_{10}H_{13}]^-$. While an *endo*-H (at B9) is missing in **11** (compare **9**), bridge hydrogen atoms are known to be more acidic than terminal hydrogens. Accordingly, structures **15b** and **16b** derived by removing the B5/B10 bridging hydrogen atom from **9b** and **10b**, respectively, are considerably more stable than the proposed $[LB_{10}H_{12}]^{2-}$ structure **11** (by 41.6 and 33.5 kcal mol^{-1}, respectively). However, both **15b** and **16b** are still unbound with respect to isolated $[B_{10}H_{12}]^{2-}$ (**26**) and NH_3 (by 14.6 and 22.7 kcal mol^{-1}). The *endo* isomer **16b** is more stable than **15b** (by 8.1 kcal mol^{-1}), partially because the former benefits from an intermolecular hydrogen bonding between the positively charged H atom bound to N and the negatively charged *endo*-H at B9 (the H···H distance is 1.556 Å).[23] For L's without positively charged hydrogens, the *endo* isomer (**16**) has no energetic advantage over the *exo* (**15**): **15a** is lower in energy than **16a** by only 2.8 kcal mol^{-1}. Bulky substituents probably will favor the *exo* over the *endo* position. Averaged chemical shifts computed for structures **12**−**17** do not fit the NMR data measured for $M_2[B_{10}H_{12}]$ in solution.[5]

The computational results suggest that complex formation of $[B_{10}H_{12}]^{2-}$ with solvent molecules is not important. Free $[B_{10}H_{12}]^{2-}$ may be the predominant species in solution, instead. We note that we do not address the issue of yellow $[B_{10}H_{12}]^{2-}$ solutions, which were attributed without further evidence to "loose solvent−$B_{10}H_{12}{}^{2-}$ complex formation".[5] Before discussing the $[B_{10}H_{12}]^{2-}$ dianion, we first clarify the solution structure of the $[B_{10}H_{13}\ ]^-$ monoanion.

$[B_{10}H_{13}]^-$. *nido*-$B_{10}H_{14}$ (**17**; see Figure 5) is easily deprotonated to give the $[B_{10}H_{13}]^-$ monoanion.[24] On the basis of

---

(23) For hydrogen bonds with element−hydride bonds as proton acceptors, see: Crabtree, R. H.; Siegbahn, P. E. M.; Eisenstein, O.; Rheingold, A. L.; Koetzle, T. F. *Acc. Chem. Res.* **1996**, *29*, 348.

(24) Guter, G. A.; Schaeffer, G. W. *J. Am. Chem. Soc.* **1956**, *78*, 3456.

Table 5. ^{11}B Chemical Shifts (ppm) for Different $[B_{10}H_{13}]^-$ Structures

	B1	B2	B3	B4	B5	B6	B7	B8	B9	B10
19, C_1, MIN[a]	7.3	−46.2	−4.5	−31.0	−8.5	−9.2	−2.5	−6.5	21.9	−5.9
19, av	7.3	−38.6	−4.5	−38.6	−7.2	9.7	−4.5	−4.5	9.7	−7.2
18, C_s, MIN[a]	−3.7	−24.6	−21.2	−24.6	−30.2	11.1	4.7	4.7	11.1	−30.2
21, C_1, TS[a]	−1.7	−31.3	−16.6	31.6	−38.4	12.8	−3.2	4.4	7.9	−10.1
20, C_s, TS[a]	−0.1	−37.0	−0.1	−31.9	−13.5	3.4	−13.5	32.8	−15.5	32.8
experiment[b]	*2.5*	*−35.2*	*−5.0*	*−35.2*	*−5.0*	*6.8*	*−5.0*	*−5.0*	*6.8*	*−5.0*
experiment[c]	*1.5*[d]	*−35.8*	*−5.7*[d]	*−35.8*	*−5.7*	*5.9*	*−5.7*	*−5.7*	*5.9*	*−5.7*

[a] MIN = minimum, TS = transition structure. [b] $[NHEt_3][B_{10}H_{13}]$ in CH_2Cl_2; ref 25. [c] $[NHEt_3][B_{10}H_{13}]$ in CH_2Cl_2; ref 26. [d] Experimentally, B1 and B3 could not be assigned unequivocally.

Table 6. ^{11}B Chemical Shifts (ppm) for Different $[B_{10}H_{12}]^{2-}$ Structures

	B1	B2	B3	B4	B5	B6	B7	B8	B9	B10
22, C_{2v}	−2.2	−35.6	−2.2	−35.6	18.2	−16.3	18.2	18.2	−16.3	18.2
23, C_{2v}	−19.4	−33.2	−19.4	−33.2	−29.5	28.3	−29.5	−29.5	28.3	−29.5
24, C_s	−24.5	−49.5	−24.5	−7.6	−10.5	−42.0	−10.5	−23.7	50.3	−23.7
24, C_s, av	−24.5	−28.5	−24.5	−28.5	−17.1	4.2	−17.1	−17.1	4.2	−17.1
25, C_1	−9.0	−36.1	−36.5	−10.8	−27.9	−34.5	4.8	2.6	26.6	−22.5
25, C_1, av	−22.7	−23.4	−22.7	−23.4	−10.8	−3.9	−10.8	−10.8	−3.9	−10.8
26, C_2	−4.5	−41.7	−4.5	−41.7	−12.0	4.4	−5.9	−12.0	4.4	−5.9
26, C_2, av	−4.5	−41.7	−4.5	−41.7	−8.9	4.4	−8.9	−8.9	4.4	−8.9
27, C_s	1.2	−39.6	−18.4	−39.6	−9.7	8.5	−5.5	−5.5	8.5	−9.7
27, C_s, av	−8.6	−39.6	−8.6	−39.6	−7.6	8.5	−7.6	−7.6	8.5	−7.6
30, C_1, TS	−11.4	−25.2	−5.6	−33.4	−18.2	21.7	−13.1	13.1	−30.7	32.8
experiment[a]	*−5.2*	*−35.6*	*−5.2*	*−35.6*	*−6.8*	*5.3*	*−6.8*	*−6.8*	*5.3*	*−6.8*

[a] For $Na_2[B_{10}H_{12}]$ in MeCN, values have been estimated from the spectrum shown in ref 5. The values reported for $[Ph_4As][B_{10}H_{12}]$ in ref 4 are as follows (without assignment; intensities in parentheses): −40.60 (1), −36.2 (1), 31.3, −25.9, −19.7 (total of 5), −6.65 (2), −1.44 (1).

the ^{11}B NMR spectrum for $[Et_3NH][B_{10}H_{13}]$ (four doublets of intensities 2:1:5:2; see Table 4), Siedle et al. proposed a static C_s structure with B5/B10, B6/B7, and B8/B9 H-bridges (**18**; Figure 5).[25] The authors pointed out that a rapid hydrogen exchange on only one side of the cluster (between the B5 and B6 and the B9 and B10 bridging positions) also would be in line with the NMR observations.

Hermánek et al. studied the acidity of decaborane(14) and benzyl derivatives and also speculated on the $[B_{10}H_{13}]^-$ structure.[26] They consider the ^{11}B NMR spectra to be "in mediocre agreement" with a fluxional C_1 structure (**19**; Figure 5), to disagree with **20** (with its *endo*-H at B9 and hydrogen bridges between B5 and B6 and between B6 and B7; Figure 5), but to be in good accord with the static C_s (**18**) favored by Siedle et al.[25] Sneddon et al.[27] were able to show that $[B_{10}H_{13}]^-$ has a C_1 symmetric structure (**19**) in the solid state, and geometric data from an X-ray investigation on the $[PhCH_2NMe_3]$ salt were published by Wynd and Welch in 1989.[28] Todd and Siedle reported that "in the ^{11}B NMR spectrum of $Na[B_{10}H_{13}]$ in diethyl ether, the −5 ppm region consists of two overlapping doublets of relative areas 2:3. The resonances from B(5,10) and B(7,8) may be resolved in this case."[29] These authors also state that "a low temperature ^{1}H NMR study will be needed to determine whether the $[B_{10}H_{13}]^-$ ion is fluxional in solution and if cation or solvent effects are important."[29] We now show computationally that the solution structure is C_1 as in the solid state and explain the fluxional behavior.

Structure **18** is characterized as a minimum on the potential energy surface, but the computed chemical shifts disagree with the experimental data (see Table 5). In contrast, **19** (C_1) is 4.5 kcal mol^{-1} lower in energy and averaged chemical shifts reproduce the NMR measurements nicely. Averaging assumes facile hydrogen rearrangment from the B5/B6 to the equivalent B9/B10 bridging position which occurs via transition state **21** and the C_s symmetric intermediate **18**. The barrier is only 5.4 kcal mol^{-1}. In contrast, moving the bridging B8/B9 hydrogen to the B9/B10 position through transition structure **20** (featuring a BH_2 moiety at B9) has a much larger barrier, 15.1 kcal mol^{-1}. This explains why $[B_{10}H_{13}]^-$ seems to be C_s symmetric on the NMR time scale rather than C_1 or C_{2v}. The good agreement of measured and computed chemical shifts also demonstrate that no specific interactions with the counterion or the solvent molecules take place in solution. Note that the global minimum structure (**19**) can be derived from $B_{10}H_{14}$ by removing one bridging hydrogen atom without reordering the remaining three. The experimental solid-state structure is in good agreement with the optimized structure **19** as far as the boron cluster is concerned. The placements of the hydrogen atoms, not unexpectedly, differ somewhat. This can be quantified by MP2-(fc)/6-31G* energies of 35.3 and 0.5 kcal mol^{-1} for the X-ray structure and a partially hydrogen-optimized X-ray structure (with B placements fixed) relative to the fully optimized geometry (**19**).

$[B_{10}H_{12}]^{2-}$. The first structure proposed for $[B_{10}H_{12}]^{2-}$, C_{2v} symmetric **22**,[2] corresponds to a higher order stationary point (three imaginary frequencies at HF/6-31G*). Although 9.4 kcal mol^{-1} more stable than **22**, the C_{2v} alternative with two hydrogen bridges (B5/B10, B7/B8), **23**, also is not viable. Not only does **23** have two imaginary frequencies, but it is still 20.3 kcal mol^{-1} higher in energy than the best $[B_{10}H_{12}]^{2-}$ (**26**). Chemical shifts computed for **22** and **23** do not fit the experimental data reported by Gaines et al.[5] Hence, $[B_{10}H_{12}]^{2-}$ adopts a lower symmetry structure. Removing another bridge hydrogen atom from the C_1 $[B_{10}H_{13}]^-$ minimum **19**, gives three $[B_{10}H_{12}]^{2-}$ candidates, **24**, **26**, and **27**.

---

(25) Siedle, A. R.; Bodner, G. M.; Todd, L. J. *J. Inorg. Nucl. Chem.* **1971**, *33*, 3671.

(26) Hermánek, S.; Plotová, H.; Plesek, J. *Collect. Czech. Chem. Commun.* **1975**, *40*, 3593.

(27) Sneddon, L. G.; Huffman, J. C.; Schaeffer, R. O.; Streib, W. E. *J. Chem. Soc., Chem. Commun.* **1979**, 474.

(28) Wynd, A. J.; Welch, A. J. *Acta Crystallogr.* **1989**, *C45*, 615.

(29) Todd, L. J.; Siedle, A. R. *Prog. NMR Spectrosc.* **1979**, *13*, 87.

(30) Hermánek, S. *Chem. Rev.* **1992**, *92*, 325.

Structure **24**, obtained by deprotonating the B8/B9 hydrogen bridge in **19**, is a transition structure at HF/6-31G*. The corresponding C_1 minimum **25** has almost the same energy (the relative energy is 0.5 kcal mol^{-1} when the zero-point energy correction is included). However, neither **24** nor **25** is relevant for the $[B_{10}H_{12}]^{2-}$ solution structure since the averaged computed ^{11}B chemical shifts do not agree with the experimental values.

Removing the B6/B7 bridging H from **19** gives the C_2 symmetric **26**. This not only is a minimum on the potential energy surface but also is the lowest energy $[B_{10}H_{12}]^{2-}$ structure we have located. Averaged chemical shifts computed for **26** match Gaines' measurements reasonably well. This agreement also confirms the 1995 experiments[5] and further discredits the data reported in 1975:[4] none of our $[B_{10}H_{12}]^{2-}$ geometries reproduce the ^{11}B chemical shifts of ref 4 (Table 6).

The agreement of ^{11}B NMR chemical shifts obtained from computations with experiment is also satisfactory for an alternative C_s symmetric doubly bridged $[B_{10}H_{12}]^{2-}$ structure **27** (with bridging H's between B6 and B7 and between B8 and B9). As **27** is 4.7 kcal mol^{-1} higher in energy, we believe that **26** is the only important structure of $[B_{10}H_{12}]^{2-}$ in solution. This $[B_{10}H_{12}]^{2-}$ minimum (**26**) can be derived from $B_{10}H_{14}$ (**17**) by removing two opposite bridging protons (B6/B7 and B9/B10 or B5/B6 and B8/B9).

Rapid migration of the B5/B6 bridge into the B9/B10 bridging position and of the B8/B9 bridging hydrogen to the B6/B7 edge results in effective C_{2v}, symmetry for $[B_{10}H_{12}]^{2-}$ on the NMR time scale. The relative energies of transition structure **28** and of intermediate **29** are 4.9 and 3.1 kcal mol^{-1}, respectively. As with $[B_{10}H_{13}]^{-}$, the rearrangment of one bridge hydrogen atom from B8/B9 to B9/B10 in **26** has a much higher barrier. The corresponding transition state, **30**, with a BH_2 moiety at B9, has a relative energy of 12.3 kcal mol^{-1}.

Conclusions

The ab initio/IGLO/NMR method[7] shows prior structural proposals for several boron hydrides to be incorrect. $[B_{10}H_{12}]^{2-}$ has been suggested[5] to form adducts with solvent molecules L in solution. However, a static, C_{2v} symmetric $[6,9\text{-}L_2B_{10}H_{12}]^{2-}$ (**1a**, L = HCN; **1d**, L = MeCN) was found to be a higher order stationary point much higher in energy than two L and $[B_{10}H_{12}]^{2-}$ at HF/6-31G* (149 and 155 kcal mol^{-1} for **1a** and **1d**, respectively).

An alternative hypothesis suggested to explain the experimental NMR observations, namely, a rapid equilibrium between $[6\text{-}LB_{10}H_{12}]^{2-}$ and L + $[B_{10}H_{12}]^{2-}$, also is refuted by our computational results: C_s and C_1 symmetric [*exo*-6-$LB_{10}H_{12}]^{2-}$ structures (**11a,b**, **15a,b**, and **16a,b**) are much higher in energy than $[B_{10}H_{12}]^{2-}$ + L. In addition, ^{11}B NMR chemical shifts computed for various $[LB_{10}H_{12}]^{2-}$ and $[L_2B_{10}H_{12}]^{2-}$ structures all deviate strongly from the data measured for $[B_{10}H_{12}]^{2-}$ in solution.[5] The most stable $[B_{10}H_{12}]^{2-}$ structure we could find (**26**, with C_2 symmetry and two hydrogen bridge atoms between B5 and B6 and between B8 and B9) results in computed chemical shifts which are in good agreement with the experimental NMR data. Hence, the $[B_{10}H_{12}]^{2-}$ solution structure (**26**) can be derived from $B_{10}H_{14}$ (**17**) by removing two opposite bridge protons without rearranging the remaining hydrogen atoms or adding Lewis bases.

Similarly, the C_1 $[B_{10}H_{13}]^{-}$ minimum, **19**, is isostructural with $B_{10}H_{14}$ (**17**), but with one bridge hydrogen atom missing. The alternative C_s isomer, **18**, with reordered H-bridges (B5/B10, B6/B7, and B8/B9), is an intermediate in the hydrogen-scrambling process. This has a barrier of only 5 kcal mol^{-1} and accounts for the effective C_s symmetry found in NMR studies.

The proposed $[6,6\text{-}(py)_2B_{10}H_{12}]$ constitution (**8d**)[20] is challenged by comparison of computed and reported ^{11}B NMR chemical shifts. For various ligands L (L = HCN, NH_3, py), the $[6,6\text{-}L_2B_{10}H_{12}]$ constitution is ca. 30 kcal mol^{-1} less stable than the *exo*-6,*exo*-9-$L_2B_{10}H_{12}$ isomers.

Acknowledgment. Financial support by the Deutsche Forschungsgemeinschaft (Schwerpunktprogramm Polyeder) and the Fonds der Deutschen Chemischen Industrie is gratefully acknowledged.

Supporting Information Available: Listings of absolute energies and of Cartesian coordinates for optimized geometries (25 pages). Ordering information is given on any current masthead page.

IC9805729